

## PERFORMANCE ESTIMATES FOR THE UPGRADED SINQ COLD SOURCE

F. Atchison

*During the coming shutdown 2003, the SINQ liquid Deuterium cold neutron source is to be replaced with a new version that includes a single re-entrant beam window on the neutron guide-system side. This should nearly double the intensity in the guide system at long wavelengths.*

### INTRODUCTION

The nub of SINQ is a spallation target at the centre of an  $\approx 5 \text{ m}^3$  tank of heavy water. The fast neutrons produced in the target by interactions of 590 MeV protons are slowed down (moderated) by scattering on the Deuterons of the heavy water until they come into thermal equilibrium. These neutrons have a Maxwell-Boltzmann energy distribution with a characteristic energy roughly equal to the physical temperature of the heavy water ( $30 \text{ C} = 26 \text{ meV} = 1.8 \text{ \AA}$ ).

For neutron scattering experiments, lower energy (longer wavelength) neutrons, say in the region 4 to 10  $\text{\AA}$ , are especially useful and the neutron intensity in this region can be enhanced by introducing a relatively small volume of cold moderating material into the heavy water moderator.

### THE PRESENT COLD SOURCE

The SINQ cold source consists of about 20 litres of liquid Deuterium at a temperature of  $\approx 25 \text{ K}$ . Thermal neutrons entering the source are able to transfer energy to the cold Deuterium and hence leave the source with a lower energy.

**Geometry:** The highest cold fluxes will come from as large a volume source as possible, mounted in the region where the thermal flux is highest. However, a compromise has to be made between neutronic performance and heat load on the cryogenic system. The source is mounted in a 'T' beam-tube assembly (Fig. 1), with its front face about 25 cm from the target axis. It is viewed from both sides by tangential beam tubes (the guide-system is to the right) with their axes 12 cm from the front of the liquid deuterium (i.e. at a radius of 37 cm from the target).

**Power deposition:** The heating of SINQ components is caused by the cascade of nuclear particles produced by the proton beam interacting in the target. The actual heat load comes from four sources (i) medium energy neutrons (from the target), (ii) fast neutrons, (iii) gamma-rays from the target and (iv) capture gamma rays from nearby structure material. All but the first of these vary with the type of target being operated. The actual power deposited will depend on details of the geometry and material; this is somewhat complicated in the case of the cold source.

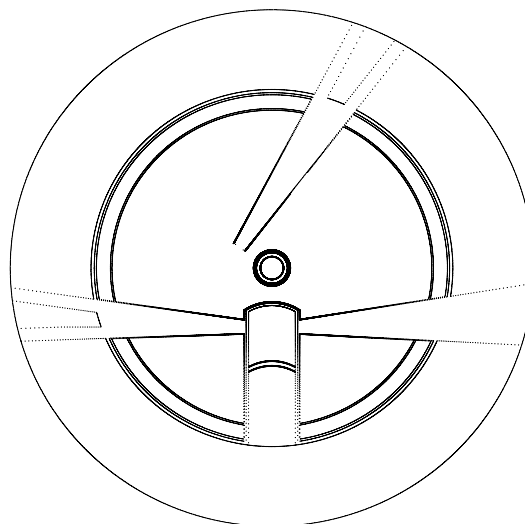


**Fig. 1:** A horizontal section through SINQ at the height of the cold source showing the cold source mounted in the T-tube assembly.

The liquid Deuterium is held in a pure Aluminium container which is mounted inside a Zircaloy vacuum tube. This, in turn, is surrounded by a cover gas contained by an Aluminium tube and the whole assembly is mounted in the radial arm of the T-tube assembly. This is shown in Fig. 2.

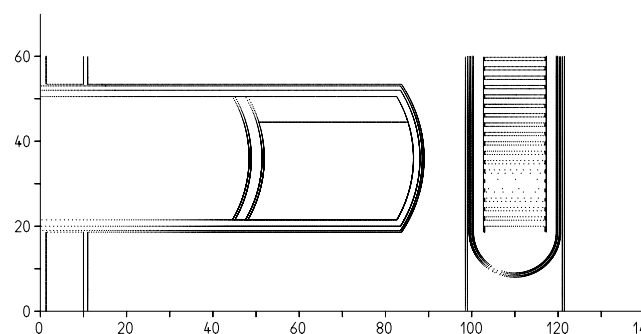


**Fig. 2:** A vertical section through the liquid Deuterium cold source and SINQ target (the figure comes from the model of SINQ used in the transport calculation).

The important heat sources are those that are to be removed by the cryogenic system; the heat load to the liquid Deuterium itself and to the walls of its container.

The calculated values for the main contributions to the cryogenic heat load are listed in Table I for operation with an ideal Pb-target (this gives the highest neutron intensities) and with the Zircaloy-rod target as used for initial operation of SINQ.

The influence of the target on the heat load varies with the particular contribution:

- a roughly constant medium energy neutron contribution,
- the fast neutron contribution is proportional to the fast neutron production and hence varies with both mass of the target nuclei and with proton energy,
- the beam- $\gamma$  component has contributions from nuclear gamma rays and from neutral pion decay (factor  $\eta$ ),
- the capture gamma component depends on the thermal neutron flux in the region of the cold source ( $\phi_{25}$ ).

The calculated heat load on the refrigerator with a Zircaloy-rod target is 540 W/mA which is about 10 % higher than the measured heat load [1] of 490 W/mA. Calculated and measured heat loads with the steel-tube cannelloni target (the one presently being used) are also in reasonable agreement; predicted, a 24 % increase to 670 W/mA and measured an 18 % increase to 580 W/mA. Heating for other target systems may be estimated using the parameters in Table 2. The predicted neutron spectrum with the Zircaloy rod target also compares well with measured values (Fig. 3).

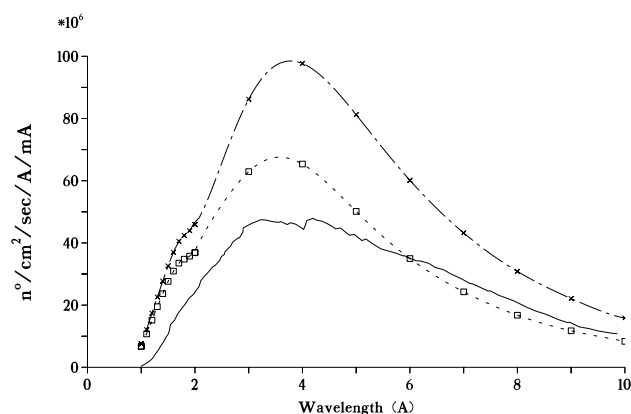


**Fig. 3:** The calculated and measured neutron spectra in the super-mirror guide =1RNR14. The solid line represents the experimental data [2] and the dashed line with squares the calculated spectrum [3]. The third curve (double-dash line with crosses) is the predicted spectrum with the re-entrant window cold source.

Target	Pb-Bi		Zircaloy-rod	
	D <sub>2</sub>	Cell	D <sub>2</sub>	Cell
Medium energy n <sup>o</sup>	280	23	280	23
Fast neutrons	190	7	70	3
Nuclear gamma rays	31	37	19	22
Capture $\gamma$ from:				
D <sub>2</sub> cell walls	87	64	20	15
Zircaloy vacuum tube	39	20	9	4
Al cover gas tube	61	33	14	8
T-tube element	30	8	7	2
Beam tube	130	61	31	14
Totals	≈ 850	≈ 250	≈ 450	≈ 90

**Table 1:** Power deposition in the SINQ cold source - Values are in W for 1 mA proton current onto target.

Target	Fast n <sup>o</sup> /p	$\eta$	$\phi_{25}$
Ideal Pb	9.16	1.0	$1.3 \times 10^{14}$
Pb-shot	7.71	1.0	$1.0 \times 10^{14}$
Pb-Zircaloy Cannelloni	6.51	1.0	$1.0 \times 10^{14}$
Pb-Bi in steel container	7.94	1.0	$8.5 \times 10^{13}$
Pb-Steel Cannelloni	6.51	1.0	$7.0 \times 10^{13}$
Zircaloy rod	3.48	0.6	$5.2 \times 10^{13}$

**Table 2:** Parameters for various target options.

## THE UPGRADED COLD SOURCE

The upgraded cold source is to be equipped with a re-entrant beam window on the neutron guide side. The basic physics of the moderating process tells us that the maximum flux is at the centre of the source (there is no incoming cold spectrum so there has to be a flux gradient toward the outer surface of the source). In the same way that thermal beam tubes are inserted into the heavy water to allow the high neutron flux regions to be exploited, the re-entrant window probes the fluxes toward the middle of the cold source.

The re-entrant window consists of an inverted box, closed at the top, open at the bottom, of volume about 1.4 litres which traps the gas from evaporated deuterium and thereby expels the liquid thus leaving the required void. A photograph of the assembly during manufacture is included as Fig. 5 at the end of this report. The power density varies with position and with target (Table 1) and for the container walls are in the range 50 to 100 mW/g for 1 mA proton current onto an ideal Pb target. The power density in the liquid deuterium varies by a factor of about 4 across the volume. The power which will be available to boil off the liquid Deuterium (in the liquid Deuterium and in the Aluminium of the re-entrant window) are as follows for 1 mA proton beam onto the appropriate target.

	D <sub>2</sub> Total W.	mW/g in Al.
<b>Pb-target</b>	66	60
<b>Cannelloni</b>	56	50
<b>Zircaloy-rod</b>	35	20

The thickness of the material of the window assembly has to be chosen so that the window is emptied for reasonably low beam currents but the source performance is not ruined by "frothing" at the highest beam currents. The calculated gains in intensity [4] are shown in Fig. 4 and the predicted spectrum in the super-mirror guide =1RNR14 is included in Fig. 3.

The double differential neutron brightness at the surface of the cold source may be calculated from

$$I(\lambda) = 0.0163 \times \phi_{25} \times [M(1.79, \lambda) + 0.612 \times M(4.83, \lambda)] \times G(\lambda)$$

where  $M(\lambda_T, \lambda)$  is the flux-Maxwell function

$$M(\lambda_T, \lambda) = 2 \times \left( \frac{\lambda_T}{\lambda} \right)^4 \times e^{-\left( \frac{\lambda_T}{\lambda} \right)^2}$$

and  $G(\lambda)$  is the gain factor at the wavelength  $\lambda$  from the re-entrant window as shown in Fig. 4.

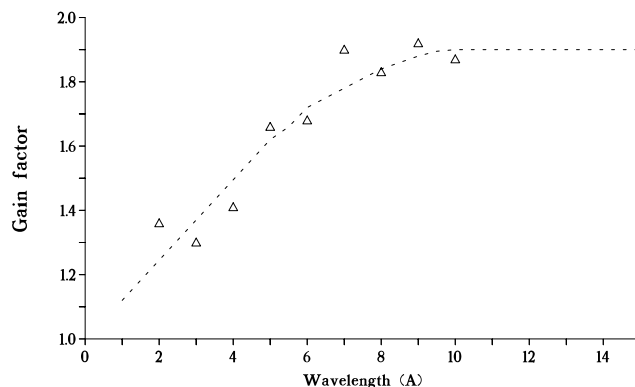


**Fig. 5:** The calculated gain factors with the re-entrant beam window as a function of wavelength. The dashed line is a guide for the eye, in particular to show the form expected at long wavelengths.

## REFERENCES

- [1] H. Spitzer, *Private Communication*, March 2000.
- [2] W. Wagner, G.S. Bauer, J. Duppich, S. Janssen, E. Lehmann, M. Lüthy, H. Spitzer, *J. Neutron Research* **6**, 249 (1998).
- [3] F. Atchison, *Calculated neutron intensities for SINQ*, PSI Report 98-03 (1998).
- [4] F. Atchison, *Some results from neutronic-calculations of the D<sub>2</sub> cold-neutron source*, SINQ project report SINQ/816/AF38-901 (1989).



**Fig. 4:** A photograph of the front section of the liquid Deuterium vessel for the upgraded SINQ cold source before final welding, showing the re-entrant beam window.

Photograph courtesy of H. Spitzer (ASQ)